Courant Institute of Mathematical Sciences

AEC Computing and Applied Mathematics Center

Helium at Zero Temperature with Hard-Sphere and Other Forces

M. H. Kalos, D. Levesque
and L. Verlet

New York University

AEC Computing and Applied Mathematics Center
Courant Institute of Mathematical Sciences
New York University

HELIUM AT ZERO TEMPERATURE WITH HARD-SPHERE AND OTHER FORCES

M. H. Kalos[*]

and

D. Levesque and L. Verlet
Laboratoire de Physique Théorique et Hautes Energies
Orsay, France[†]

Abstract

Various theoretical and numerical problems relating to helium-like systems in their ground states are treated. New developments in the numerical solution of the Schrodinger equation permit the solution of 256 body systems with hard-sphere forces. Using periodic boundary conditions, fluid and crystal states can be described; results for the energy and radial distribution functions are given. A new method of correcting for low lying phonon excitations so as to extrapolate the energy of fluids to an infinite system is described. A perturbation theory relating the properties of the system with pure hard sphere forces to those with smoother, more realistic two body forces is introduced. As in recent work on classical systems the potential is divided into two continuous parts; one is repulsive, one attractive, the latter being treated as a perturbation. The solution for the repulsive part is taken directly from the hard sphere problem when the radius is identified as the scattering length of the repulsive part of the smooth potential. The convergence for the Lennard-Jones potential is very good. Using our numerical results for the hard sphere problem, with phonon corrections, together with this perturbation theory, results for energy vs. density agree with experiment within our error of 3-10% except at high crystal densities. We carry further Schiff's recent application of this perturbation theory to He^3 and conclude that antisymmetrization by the method of Wu and Feenberg is the reason for lack of agreement with experiment in that system.

1. Introduction

In this paper we investigate in some detail the properties of the ground state of the hard-sphere boson system and apply the results of this study to the real helium case at zero temperature. It is generally assumed that the significant features of the structure of liquid helium are related to the repulsive part of the interaction, the weak attraction for tne most part playing the role of keeping the system bound. A good qualitative description of helium should be contained in the hard-sphere problem. This is our first motivation to study that simple system. In view of the success of perturbation theory in the case of classical fluids where an expansion is carried out around a suitably defined hard-sphere reference system, one may try to build the same kind of perturbation theory in the case of liquid helium, where the hard-sphere properties are also essential ingredients. We shall show that such a theory can be built and that it is very simple and quantitatively successful.

The interest in the hard-sphere Bose system is, of course, not new. Bogolioubov,[1] Lee and Yang,[2] and others,[3] have given expressions for the energy of the ground state which are exact in the low density limit. These expressions

are unfortunately useless for densities of physical interest. The only existing computations in the high density domain are due to Hansen, Levesque, and Schiff[4] who use in the case of the fluid phase a variational wave function of the Bijl-Jastrow type

$$\psi_J(\vec{r}_1 \cdots \vec{r}_N) = \prod_{i<j} e^{-u(r_{ij})/2} \qquad (1-1)$$

where u is a trial function. The solid is described by multiplying the function ψ_J by a product of one-particle gaussian factors centered around the prescribed sites of the equilibrium lattice. Solving this problem numerically through the usual Monte Carlo technique used in classical statistical mechanics, HLS obtain the energy as a function of density for the liquid and solid phase, and the parameters of the first-order transition which lies between these phases.

The first part of this paper is devoted to the solution of the quantum hard-sphere problem (sections 2 through 5). This solution based on a method devised by one of us[5] is numerical but essentially exact.

In section 2 we give a summary of this numerical method. It relies on the fact that the wave function of bosons at zero temperature, and the Green's function of the Schrodinger equation written as an integral equation are positive quantities which can be used as probabilities in a Monte Carlo

computation. In the case of the hard-sphere system the only -- but very great complication -- in the Green's function lies in the complex boundary conditions imposed by the $N(N-1)/2$ conditions stating that the hard cores do not overlap. A similar Green's function can however be sampled in a practical way on simpler subdomains included in the general complex domain; one can write and solve an integral equation which makes it possible to cover the complicated large domain with the simpler subdomains and thus to build the general Green's function. The use of the Jastrow function as a biasing factor in the Monte Carlo method makes the computation feasible.

Section 3 is devoted to the construction and sampling of the Green's function in the simple subdomains.

In section 4 we give some indications of the technical aspects of the method.

The results of the computation are given in section 5. A comparison is made (Table 6) with the variational results. The energies obtained through the "exact" computation are slightly, although significantly, lower than the variational ones. In the liquid state the radial distribution functions (rdf) clearly present more structure than the variational ones. The off diagonal long range (ODLR) parameters are very slightly smaller than the corresponding variational ones.

The results of the preceding section have been calculated for a small system: 256 in our study. In section 6

the extension to quasi-infinite systems is considered.
It requires the inclusion of long wavelength excitations
which, as is well known, play an essential role in liquid
helium. Due to these long wave length phonons the energy
of the dense fluid is lowered by about 2%. The use of
the "exact" results for the energies, with phonon corrections,
brings a displacement of the freezing and melting densities
by about 10% as compared with the results obtained varia-
tionally by HLS.

In the rest of the paper, we apply the hard-sphere
results to the case of more realistic helium-like systems.

In section 7 we introduce the relevant perturbation
theory. We divide the interaction $v(r)$ into two parts,
as is done for the classical liquids: a part $v_0(r)$ which
gives rise to the repulsive forces and which will be replaced
later on by hard spheres located at the scattering length
of v_0; the remainder of the interaction $w(r)$ which will
be treated as a perturbation. The numerical tests are made
using the Jastrow wave function and a Lennard-Jones potential

$$v(r) = 4\epsilon \left[\left(\frac{\sigma}{r}\right)^{12} - \left(\frac{\sigma}{r}\right)^{6} \right] \tag{1-2}$$

for which many variational computations have been made.[7-10]
The convergence of the theory is shown to be excellent.
Terms of higher than first order   contribute to the
energy below the noise level of the computation, i.e. about
0.1° K. The physical reason for this good convergence

appears to be the following. The ground state wave function of the system must be nodeless and bent as little as possible to keep the kinetic energy down. This tends to keep the particles as far away from one another as possible. In the dense fluid region this prevents large density fluctuations. The higher order terms are therefore much smaller than what they would be for a classical system for the same (not very high) density. The fact that the particles keep away from each other contrasts with the opposite situation relative to the classical system for which the radial distribution function   has a peak near the core. This makes the quantum case much simpler than the corresponding classical case where the replacement of the repulsive potential $v_0(r)$ by hard cores cannot be made without introducing some density-dependent corrections to take into account the shape of $v_0(r)$. Here these corrections may be neglected; the density-independent diameter is obviously the scattering length a of the potential $v_0(r)$. To first order, the energy of the total system is simply given as

$$\frac{E}{N} = \frac{E_H(\rho a^3)}{N} + \frac{\rho}{2} \int d\vec{r} \ w(r) \ g_H(r) \qquad (1-3)$$

where E_H and g_H are respectively the energy and the rdf of hard spheres of density ρ and diameter a. The theoretical justification of this perturbation theory is examined in section 8.

We then make (section 9) a digression on the variational problem in the case of continuous potentials: the perturbation theory suggests a form of the Jastrow wave function closely related to the hard-sphere one and very different from the trial function usually used in the LJ case. We show that despite this difference this wave function yields the usual value, of the order of -5.8°K for the energy, and an rdf which presents a little more structure than the ones previously obtained.

In section 10 we give the results obtained with the perturbation theory. We first show that using the variational hard-sphere results obtained with the HLS trial function, one recovers the LJ variational energies both for the liquid and the not too dense solid phase. This shows the very large degree of success of the perturbation theory. We then introduce the "exact" results for the fluid with the phonon correction included. This has the effect of lowering the energy of the liquid by about 0.6° and of bringing the location of the minimum of the energy versus density and the transition data into essential agreement with experiment.

In the last section (section 11) we extend to the quantum case the hard-sphere model introduced in the classical case in order to describe the structure factor obtained from X-ray and neutron scattering experiments.

Appendix A is devoted to a tabulation of the numerical results for the radial distribution function.

In Appendix B, we make some remarks on the problem of He^3 which complement the recent study by Schiff.[12]

2. Monte Carlo Integration of the Schrodinger Equation

We write the Schrodinger equation for a system of bosons interacting by hard core forces in the following dimensionless form (with $\hbar^2/2m = 1$, potential radius = a):

$$- \sum_i \nabla_i^2 \psi(\vec{r}_1,\ldots,\vec{r}_N) = E\psi(\vec{r}_1,\ldots,\vec{r}_N) \qquad (2.1)$$

with the boundary conditions

$$\psi(\vec{r}_1,\ldots,\vec{r}_N) = 0 \quad \text{when} \quad |\vec{r}_i-\vec{r}_j| \leq a \quad \text{for all } i \neq j \qquad (2.2)$$

In addition, the wave function is periodic in a box of side $L = (N/\rho)^{1/3}$:

$$\psi(\vec{r}_1,\ldots,\vec{r}_i,\ldots,\vec{r}_N) = \psi(\vec{r}_1,\ldots,\vec{r}_i+\vec{p}_j,\ldots,\vec{r}_N) \quad ,$$

$$\vec{p}_j = L \times \text{unit vector in x,y or z directions,}$$
$$i = 1,\ldots,N,$$

Equation (2.1) is written in the succinct form

$$- \nabla^2 \psi(R) = E\psi(R) \qquad (2.3)$$

Now suppose $G(R,R_0)$ satisfies

$$- \nabla^2 G(R,R_0) = \delta(R-R_0) \qquad (2.4)$$

Equation (2.3) may be rewritten as

$$\psi(R) = E \int G(R,R') \psi(R') \, dR' \qquad (2.5)$$

If a succession of functions is defined by

$$\psi^{(n+1)}(R) = E \int G(R,R') \, \psi^{(n)}(R') \, dR' , \qquad (2.6)$$

$$n = 0,1,\ldots$$

then the ground state ψ_0 of equation (2.1) is the asymptotic $\psi^{(n)}$ for large n. The Monte Carlo method consists in sampling possible sets of coordinates $\{R_0\}$ at random from $\psi^{(0)}$, an initial or trial function. For any point R_n drawn from $\psi^{(n)}(R_n)$, a point R_{n+1} drawn from $\psi^{(n+1)}$ is obtained by sampling $E \, G(R_{n+1},R_n)$ considered as a density function for R_{n+1} conditional upon R_n. We will call a set of coordinates R a "configuration" and refer to the population of configurations with a given value of n as a "generation".

E_0 , the energy of the ground state, is that value of E which makes the normalization of $\psi^{(n)}$ (i.e., the size of the population after G has been used n times) asymptotically stable. After the process has been judged to converge, based upon estimates of E_0 and other computed results, E_0 may be determined from

$$\bar{E}_0 = E' \int \psi^{(n)} \, dR \, / \int \psi^{(n+1)} \, dR \qquad (2.7)$$

where E' is a trial value of E_0 used in the sampling.

This process may be made computationally more efficient -- to an arbitrary degree -- by the following transformation. Let $\psi_J(R)$ be a trial function which may be the same as $\psi^{(0)}(R)$. Then let

$$\tilde{\psi}(R) \;=\; \psi_J(R)\,\psi(R) \tag{2.8}$$

Equation (2.5) becomes

$$\tilde{\psi}(R) = E' \int [\psi_J(R)\,G(R,R')/\psi_J(R')]\;\tilde{\psi}(R')\;dR'\;, \tag{2.9}$$

formally the same as (2.5). A sequence of functions obtained by successive application of G to $\psi_J(R)\psi^{(0)}(R)$ converges to $\psi_J\psi_0$ and E_0 is again that value that makes the population stable. It will be shown below that, as $\psi_J \to \psi_0$, the estimates of E_0 obtained from

$$\bar{E}_0 = E' \int \tilde{\psi}^{(n)}\;dR / \int \tilde{\psi}^{(n+1)}\;dR \tag{2.10}$$

are correct on the average at $n = 0$ (without requiring $\psi^{(0)} = \psi_0$). Furthermore E_0 may in fact be estimated with zero statistical error. One expects -- and our experience strongly supports -- that a reasonable analytical trial function ψ_J greatly reduces the computational effort required.

Unfortunately, Green's function given in Eq. (2.4) is not known owing to the complexity of the boundary conditions. But all that is required is that a scheme

be devised for sampling $G(R,R_0)$ for R at random given any R_0. This is possible in a recursive way as follows. Let D be the domain in configuration space not excluded by the hard core boundary conditions. Let D_0 be another domain wholly contained within D with R_0 in D_0. Let $G_0(R,R_0)$ satisfy (2.4) but vanish on the surface of D_0 (rather than that of D):

$$- \nabla^2 G_0(R,R_0) = \delta(R-R_0) \tag{2.11}$$

With the boundary conditions that they vanish on prescribed surfaces, these Green's functions are symmetric. Thus,

$$- \nabla^2 G(R_1,R) = \delta(R-R_1) \tag{2.12}$$

Multiply (2.11) by $G(R_1,R)$, (2.12) by $G_0(R,R_0)$ and integrate with respect to R over D_0. With the help of Green's theorem, we find

$$G(R_1,R_0) = G_0(R_1,R_0) + \int_{S_0} [-\nabla_n G_0(R,R_0)] G(R_1,R) \, dR \tag{2.13}$$

The integral on the right side is extended over the surface S_0 of D_0; the kernel is the normal derivative of G_0 which is everywhere positive. The substitution of (2.13) into itself yields a series of iterated integrals which may be sampled by the following random walk procedure.

A point is started at R_0 and moved to R' chosen at random on S_0 using $-\nabla_n G_0(R',R_0)$ as density function;

then a new domain D_1 is constructed, containing R' and a new point selected on the surface S_1. The process terminates only when a point arrives at the boundary of D since (2.11) implies

$$\int_{S_0} [-\nabla_n G_0(R',R_0)] \, dR' = 1 \qquad (2.14)$$

The full Green's function is the sum of all $G_0(R,R_n)$ for the R_n that appear in the random walk.

We must choose D_n at every stage so that G_0 is known or can be sampled and so that moves within D_n do not produce overlap of hard cores. A particularly convenient domain for the purpose is a Cartesian product of N spaces, each a sphere for one particle. The radii are chosen so as to prevent core overlap. This construction permits G_0 to be sampled in a straightforward numerical way (as seen in section 3 below). As shown in reference 5, the requirement that the wave function and hence Green's function be periodic is met by the computational device of putting back on the left of the box those particles which leak out of the right.

As it stands (2.14) is satisfied, so in that form the random walk does not terminate. The modification required for Eq. (2.9) removes this difficulty. We have from (2.13)

$$\psi_J(R_1) G(R_1,R_0)/\psi_J(R_0) = \psi_J(R_1) G_0(R_1,R_0)/\psi_J(R_0)$$

$$+ \int_{S_0} \{\psi_J(R) [-\nabla_n G_0(R,R_0)]/\psi_J(R_0) \} \{\psi_J(R_1) G(R_1,R)/\psi_J(R) \} \, dR \quad .$$
$$\qquad (2.15)$$

This has the same structure as (2.13) but a different kernel, $\{\psi_J[-\nabla_n G_0(R,R')]/\psi_J'\}$ for which (2.14) does not hold. In fact, if

$$-\nabla^2 \psi_J(R) \;=\; E_J(R)\;\psi_J(R) \tag{2.16}$$

and if we multiply (2.16) by $G_0(R,R_0)$, (2.11) by $\psi_J(R)$ and integrate over D_0, we have

$$\int_{S_0} \psi_J(R)\,[-\nabla_n G_0(R,R_0)]/\psi_J(R_0)\;\mathrm{d}R$$

$$= 1 - \int [E_J(R)\,\psi_J(R)\;G_0(R,R_0)/\psi_J(R_0)]\;\mathrm{d}R \tag{2.17}$$

Thus, if $E_J(R)$, a "local energy", is everywhere positive, the norm on the left, which gives the probability at R_0 that the random walk continues, is now less than 1.

Note also that if $E_J(R)$ is replaced by E, then the integral on the right in (2.17) is that contribution to

$$\int [\psi_J\;G(R,R')/\psi_J']\;\tilde{\psi}(R')\;\mathrm{d}R' \;,$$

the right side of (2.9), which comes from G_0 alone. Thus, when ψ_J is the exact eigenfunction, the process of contributing to the next generation and that of going on with the random walk which develops G may be treated as mutually exclusive random events. Then the random walk always gives exactly one configuration in the next generation and the generation size has no sampling error.

Finally we observe that Eq. (2.17) is correct if G_0 is replaced by G and the domain of integration is D.

Then, since $\psi_J = 0$ on the boundary,

$$\psi_J(R_0) = \int E_J(R) \, \psi_J(R) \, G(R,R_0) \, dR \; . \tag{2.18}$$

Again, if $-\nabla^2 \psi_J = E_0 \psi_J$,

$$E_0 = \frac{1}{\int [\psi_J(R) G(R,R_0)/\psi_J(R_0)] \, dR} \tag{2.19}$$

If, in Eq. (2.10) we set $E' = 1$ and $\psi^{(n)} = \delta(R-R_0)$, then the expected value of the integral in the denominator of (2.10) is that of (2.19); the expected energy is identically E_0, independent of R_0. Taken together with the result stated in the preceding paragraph, we see that when ψ_J is the exact eigenfunction, the energy is obtained with neither statistical nor convergence error. Expectation values are obtained by the method given in ref. 5 in which the asymptotic size of the generations which arise from a configuration at R_0 gives an estimate of $\psi(R_0)$ which is statistically independent of the sampling that led to R_0. When ψ_J is exact, the estimate of the asymptotic size is carried out with no sampling error.

The numerical calculations whose results are given below were carried out with $\psi_J(R)$ in the form suggested by Hansen, Levesque and Schiff[4]

$$\psi_J(R) = \prod_{i<j} \tanh \left((r_{ij}^m - 1)/b^m \right) \tag{2.20}$$

for the fluid, and

$$\psi_J(R) = \exp\left\{-\frac{1}{2} A \sum_i (r_i - s_i)^2\right\} \prod_{i<j} \tanh\left((r_{ij} - 1)/b^m\right)^m \quad (2.21)$$

for a crystal whose lattice sites are s_i. The
parameters b, m, and A were those used in the calculations
of ref. 4. Computational experience shows that the values
which minimize the energy in a variational calculation are
good ones for our purposes.

3. <u>Construction and Sampling</u> G_0 <u>in Product Spaces</u>

In the section above it is assumed that at any stage in the random walk, $G_0(R,R_m)$ can be sampled for some convenient domain D_m containing R_m. This is particularly simple to carry out if D_m is a Cartesian product of subspaces. We consider the case where

$$D_m = d_1 \otimes d_2 \otimes \ldots \otimes d_N \qquad (3.1)$$

and each d_k is a domain of the coordinates of the kth particle of the system. The method holds equally for other decompositions; division into relative and center of mass coordinates may be worth considering in some problems.

Let $g(r_k,r_k',t)$ satisfy

$$-\nabla^2 g(r_k,r_k',t) + \frac{\partial}{\partial t} g(r_k,r_k',t) = 0 \qquad (3.2)$$
$$g(r_k,r_k',0) = \delta(r_k-r_k')$$

and

$$g(r_k,r_k',t) = 0$$

for r_k on ∂d_k , the boundary of d_k , and outside d_k . Then for R and R' in D, set

$$G_0(R,R') = \int_0^\infty \prod_k g(r_k,r_k',t) \, dt \qquad (3.3)$$

Clearly

$$\left\{ - \sum_k \nabla_k^2 + \frac{\partial}{\partial t} \right\} \prod_k g(r_k, r_k', t) = 0 \qquad (3.4)$$

and

$$\prod_k g(r_k, r_k', 0) = \delta(R-R') . \qquad (3.5)$$

$G_0(R,R')$ vanishes for R on ∂D (some r_ℓ on ∂d_ℓ). Integrating (3.4) with respect to time and using (3.5) we find the result that

$$\left\{ - \sum_k \nabla_k^2 \right\} G_0(R,R') = \delta(R-R') \qquad (3.6)$$

as required.

In the form (3.3), sampling G_0 very nearly requires only sampling $g(r_k, r_k', t)$ for a move from r_k' to r_k for every particle. Consider the problem of sampling the normal derivative

$$-\nabla_n G_0(R,R') \qquad \text{for} \quad R \in \partial D .$$

Now

$$\partial D = \bigsqcup_m d_1 \otimes d_2 \otimes \ldots \otimes \partial d_m \otimes \ldots \otimes d_N . \qquad (3.7)$$

Sampling the kernel means first finding m, then sampling points r_ℓ ($\ell \neq m$) on the interior of d_ℓ and r_m on the surface ∂d_m. Corresponding to (3.7),

$$-\nabla_n G_0(R,R') = \sum_m \int \left[\prod_{\ell \neq m} g(r_\ell, r_\ell', t) \right] [-\nabla_n g(r_m, r_m', t)] \, dt . \qquad (3.8)$$

Let

$$H_\ell(t) = \int_{d_\ell} g(r_\ell, r_\ell', t) \, dr_\ell \qquad (3.9)$$

$$H(0) = 1$$

$$H(\infty) = 0 .$$

16

Green's theorem applied to (3.4) shows that

$$-H_\ell'(t) = -\frac{\partial H_\ell(t)}{\partial t} = \int_{\partial d_\ell} [-\nabla_n g(r_\ell, r_\ell', t)]\, dr_\ell > 0 \qquad (3.10)$$

Expand (3.8) into the form

$$-\nabla_n G_0(R, R') = \sum_m [-H_m'(t) \prod_{\ell \neq m} H_\ell(t)] \left[\frac{-\nabla_n g(r_m, r_m', t)}{-H_m'(t)} \right]$$

$$\times \prod_{k \neq m} \frac{g(r_k, r_k', t)}{H_k(t)}\, dt. \qquad (3.11)$$

The sampling procedure is as follows.

1. Sample t and m at random using the first quantity in brackets in (3.11)

2. Conditional on m and t, sample r_m at random on ∂d_m using kernel $(-\nabla_n g(r_m, r_m', t)/(-H_m'(t))$.

3. Using the same t, sample for every $k \neq m$ a point r_k in d_k using kernel $g(r_k, r_k', t)/H_k(t)$.

The function $g(r_k, r_k', t)$ describes the diffusion of a particle started at r_k' at t = 0. $H_k(t)$ is the probability that it is absorbed at the boundary of d_k after time t and $-H_k'(t)$ is the rate of absorption at t. Suppose for each k, t_k is drawn at random from the probability density function $-H_k'(t)$. The probability that the smallest of all t_k is t_m and that t_m lies in a unit interval of time near t is

17

$$- H'_m(t) \cdot \prod_{k \neq m} H_k(t) \quad .$$

In other words the operations of selecting the smallest of k values t_k, samples m and t as required for equation (3.11).

Sampling $G_0(R,R')$ itself can be done in an analogous way. Of course, all r_k lie on the interior of the corresponding domains d_k. Here a numerical approximation to $\prod_k H_k(t)$ is used to sample a value of t.

In practice, each domain d_k was taken to be a sphere of radius a_k centered at r'_k. In terms of $z_k = |r_k - r'_k|$ the familiar method of separation of variables and eigen-function expansion gives

$$g(z_k, t) = (2a_k^2 z_k)^{-1} \sum_j j \sin (\pi j z_k/a_k) \exp (- \pi^2 n^2 t/a_k^2)$$
(3.12)

We see explicitly that $a_k^3 g$ is the same function of the reduced coordinates z_k/a and t/a_k^2. This fact is exploited in the numerical work.

The expansion (3.12), and a complementary one obtained from the Poisson sum rule which converges rapidly for short time, are the basis for various numerical algorithms used to sample t_k, z_k and so on. For the most part the z_k are sampled from multivariate normal distributions which can be done efficiently. Although the procedure may seem somewhat elaborate, the computation time is dominated by the usual calculation of the distances between particles.

4.   <u>Implementation of a Computer Program</u>

We give here some technical details of the computer program in which the ideas outlined in the preceding section have been realized. Readers interested only in the theory may skip this part of the paper.

In any many body simulation a crucial detail lies in calculating the distances between pairs of particles. In the present calculation this is done for two reasons. First and most important, it is necessary to know for each particle the distance to its nearest neighbor so as to permit the choice of the sphere in which it may move without core overlap. Second, the computation of the value of the trial function ψ_J used to accelerate the computation requires the value of r_{ij} for all pairs (cf. eq. (2.20)). For the latter purpose ψ_J need not be as accurate at large pair separations as needed for good variational calculations. Hence the tabulation of r_{ij} is truncated at a distance where the hyperbolic tangent in (3.20) nearly attains the value 1. The pair function is smoothly extrapolated to 1 at that distance.

The tabulation of the pair distances follows the proce-dures that have been in use in the Orsay Monte Carlo and molecular dynamics programs for some time. It suffices to say here that tables are established in which rather near neighbors of each particle are identified. Most of the time (for a crystal, all of the time) distances are computed for pairs only in this table. When the tables

are built up or renewed at appropriate intervals, all pairs are examined.

As has been suggested in the preceding section, numerical tables are generated to facilitate sampling at random from various probability distributions required to select steps from the Cartesian product Green's function. Space limitation precludes a detailed description of the organization of these tables, their use, and the analysis that underlies them. We remark only that care was taken that with the help of these tables, the mappings or inverse mappings based on the Green's function are very rapid and accurate. With respect to the latter, extensive numerical tests showed that in a step drawn from the Green's function as kernel, the error in the mean square displacement is at most a few parts in 10^5.

The computer program has undergone considerable development during the period when it was being used. The part which has changed most is that pertaining to "importance sampling," i.e. the transformation of the dependent variable from ψ to $\psi_J \psi$ as indicated in equations (2.8) et seq. In fact, in the first version, this was not done although the role of the trial function in forcing convergence of the Green's function development was recognized and included (as in eq. (2.15)). We estimate that making the transformation in a thorough going way reduced the computer time required by about a factor of twenty.

In any case it becomes necessary to sample the kernels

$$\psi_J(R) \; [-\nabla_n G_0(R,R_0)] \; / \; \psi_J(R_0) \qquad (4.1)$$

and

$$\psi_J(R) \; G_0(R,R_0) \; / \; \psi_J(R_0)$$

rather than $-\nabla_n G_0$ and G_0 respectively. The techniques for doing this have also evolved. At present the method is based upon an expansion of $\psi_J(R)$ about $\psi_J(R_0)$. To first order

$$\psi_J(R)/\psi_J(R_0) = 1 + (R-R_0)\cdot[\nabla\psi_J(R_0)]/\psi_J(R_0). \quad (4.2)$$

If we write

$$\psi_J(R) \; = \; \exp \; (- \; u(R)) \; ,$$

then

$$\psi_J(R)/\psi_J(R_0) = 1 - (R-R_0)\cdot\nabla u(R_0) \; . \qquad (4.3)$$

$u(R)$ is commonly called the "pseudopotential"; we may refer to $-\nabla u$ as the "pseudoforce".

If ψ_J is set equal to a constant then for each sphere the direction in which a particle move is made must be chosen in an isotropic way. The pseudoforce defines a favored direction and a degree of anisotropy for the proposed move. For a system of 256 particles in a crystal phase this elementary use of the pseudoforce has reduced the required computing time by about a factor of 10. The extra time to compute the pseudoforce is included. It is clear that further improvements, possibly resulting in additional drastic savings, can be made. [11]

An awkward feature of the computational method lies
in the necessity to use a trial eigenvalue and the role
that it plays in the branching of configurations.
It appears to require one to two hundred generations
for the energy and other quantities to settle down. Since
the energy changes by a total of 3 - 8% and since the
growth of the population in n generations is proportional
to the nth power of the trial energy, the management of
the calculation in the face of statistical uncertainties
can be serious. In practice runs are made using from 10
to 80 generations; early in the relaxation process one
aims for short runs. At the end of each such run the
coordinates specifying the configurations are recorded
on magnetic tape and used as input for the subsequent run.

A recent series of runs (crystal, $\rho a^3 = 0.4$) is
typical. The process was followed for 210 generations
from a set of configurations calculated variationally
after which an additional 240 generations were followed
during which the calculated parameters were constant within
apparent errors (< 1% for the energy). A total of 21 hours
of time on a CDC 6600 was used, about 8 in the early phase.
We estimate that about one third of the total time could
have been saved if the generation growth had been observed
and managed better. In part, failure to do so lies in the
circumstances under which the computer runs were made.
It is likely that if the variance which is introduced by

the branching in the Green's function development can be
further reduced, then the uncertainties which result
from the use of the trial energy will also be reduced.

5.   Results of the Integration of the Schrodinger Equation.

The numerical results for the energy are given in Table 1. The errors quoted are estimates of the standard derivation of the Monte Carlo results of several runs (3-5) in which the properties of the system were found to be constant. In all cases the results are those for a system of 256 particles. For the fluid, a correction to an infinite system is applied as explained in the next section. Numerical values of the radial distribution function computed for the 256 body fluid both by the variational and the Schrodinger integration are given in Appendix A.

The energies are lower than those calculated variationally by a small but significant amount. In the fluid region the rdf shows slightly more structure than variational. As a consequence the main peak of the structure factor is enhanced relative to the variational prediction.

In summary, the Jastrow wave function is found to be quite good as a first approximation. The small differences will turn out, however, to be of decisive importance in the analysis that follows.

6. Taking the Phonons into Account

The approach we have followed is clearly unable to deal with long wavelength excitations, because of the limitation due to the size of the box. As we know the importance of these long wavelength excitations in liquid helium, we have to evaluate their effect. In the framework of the Jastrow approximation function the phonons can be taken into account by adding to the short-range pseudo-potential $u_s(r)$ of the Jastrow wave function, a Reatto-Chester[13] term

$$u_L(r) = \frac{mc}{\rho \pi^2 \hbar} \frac{1}{r^2 + k_c^{-2}} \qquad (6.1)$$

where c is the velocity of sound and k_c^{-1} a wavelength cutoff which should be of the order of a few interparticle distances ($.25/\sigma$ is a guess usually met in the literature). The change in the kinetic energy of the hard spheres is the sum of two terms

$$T_1 = \frac{\rho \hbar^2}{8m} \int d\vec{r} \ \nabla^2 \ u_L(r) \ g_s(r) \qquad (6.2)$$

$$T_2 = \frac{\rho \hbar^2}{8m} \int d\vec{r} \ (\nabla^2 u_s(r) + \nabla^2 u_L(r)) \ \delta g(r) \ . \qquad (6.3)$$

Here the subscript s refers to quantities calculated with the usual short range Jastrow function. $\delta g(r)$ is the change in the rdf due to the Reatto-Chester term.

The difficulty of this variational calculation is due to the long range character of the Reatto-Chester function.

It has been proposed,[14] in order to solve this problem, to use an Ewald sum technique as in the classical charged particles system. It is quite clear that we can thus take correctly into account phonons of such wave numbers which may be reached with a finite box and periodic boundary conditions. This sets a limit of 0.6 a^{-1} in the case of a 256 particle system near solidification density. If k_c is of the order of 0.2 - 0.3 a^{-1} most of the effect will be missed. We can also predict the failure of the Ewald sum technique for the following reason: in the fluid region the variational and "exact" energies do coincide within about 0.2 $\hbar^2/ma^2$. As a consequence the contribution of the short wavelength phonons is smaller than 0.2 $\hbar^2/ma^2$ and at the noise level of the standard Monte Carlo computation.

In order to tackle the problem of long wavelength phonons, we shall resort to a perturbation technique, since at least if k_c is small, we have to deal with a rather weak long-range pseudo-potential in addition to the short range function $u_s(r)$.

Defining

$$\tilde{u}_L(k) = \int d\vec{r}\; e^{i\vec{k}\cdot\vec{r}}\, u_L(r) \qquad (6.4)$$

the dominating terms in the perturbation expansion are, as is well known, the ring diagrams formed with $\tilde{u}_L(k)$ as bonds.

It has been shown[15] that the proper way of taking into account the effect of the size of the particles involved in the ring was to put at each vertex of the ring diagram the structure factor of the reference system, with no long-range pseudopotential, i.e.:

$$S_s(k) = 1 + \rho \int d\vec{r} \ (g_s(r)-1) \ e^{i\vec{k}\cdot\vec{r}} \qquad (6.5)$$

This approach leads to the formula

$$\delta g(r) = g_s(r) \ \big(\exp \ (- \ \Gamma(r)) \ - \ 1\big) \qquad (6.6)$$

with

$$\tilde{\Gamma}(k) = \frac{S_s^2(k) \ \tilde{u}_L(k)}{1+\tilde{u}_L(k) \ S_s(k)} \ . \qquad (6.7)$$

It has been noted by Andersen and Chandler[16] that $\Gamma(r)$ and thus $\delta g(r)$ depend crucially on the arbitrary assumption made on the behavior of $u_L(r)$ inside the repulsive core (where it has no physical meaning). This dependence appears only because a particular subset of graphs in the perturbation expansion has been selected. AC show that the prescription $\Gamma(r) = 0$ inside the repulsive core is very reasonable and leads to excellent results in the case of primitive models of electrolytes as well as in the case of the classical Lennard-Jones liquids.

For $\rho a^3 = 0.234$, we show in Figure 1 the energy shift as a function of k_c. It is seen that a minimum is obtained, for $k_c \simeq 0.3 \ a^{-1}$, a value which corresponds closely to the intuitive guess made above. The energy is correspondingly lowered by $0.11 \ \hbar^2/ma^2$. As this limiting wave vector is substantially smaller than the smallest wave vector considered in the actual "exact" computation ($2\pi/L \simeq 0.6 \ a^{-1}$ as we have seen) we should also apply this phonon correction to the "exact" energies given in Table

This correction on the energy, although small, has the effect of displacing the transition parameters of the hard-sphere system. Let us consider first the case of the variational computation. For the solidification density, one finds $\rho a^3 = 0.24 \pm 0.01$ instead of[4] $\rho a^3 = 0.23 \pm 0.01$. The melting density also rises from 0.25 ± 0.01 to 0.26 ± 0.01.

We now apply this phonon correction calculated in the Jastrow approximation to the "exact" results obtained in the paper. This yields the results obtained in Table 1. The final values of the energy of the hard sphere system are shown in Figure 2 as a function of $1/\rho$. A double tangent construction gives the transition parameters. We obtain for the solidification density $\rho \ a^3 = 0.25 \pm 0.01$, and for the melting density $\rho \ a^3 = 0.27 \pm 0.01$.

7. The Perturbation Expansion and Its Convergence

We shall suppose in the following that the helium atoms interact through a two-body potential $v(r)$. This is not an important restriction as the many-body forces in helium are known to be weak and can be treated as a perturbation. As in the classical theory of liquids[6] we divide the potential into two parts: a "reference" part $v_0(r)$ and a remainder $w(r)$ which will be considered as a perturbation. Let ε be the magnitude of the potential at its minimum and r_m be the corresponding abscissa. We write

$$\begin{aligned} v_0(r) &= v(r) + \varepsilon & \text{for} \quad r \leq r_m \\ &= 0 & \text{for} \quad r > r_m \ . \end{aligned} \tag{7.1}$$

We then have

$$\begin{aligned} w(r) &= -\varepsilon & \text{for} \quad r \leq r_m \\ &= v(r) & \text{for} \quad r > r_m \ . \end{aligned} \tag{7.2}$$

Let H_0 be the Hamiltonian of the reference system

$$H_0 = T + V_0 \tag{7.3}$$

where V_0 is the potential energy corresponding to the pair potential $v_0(r)$. Let ψ_0 be the normalized wave function of the ground state of the reference system, pertaining to the eigenvalue E_0. We have obviously

$$\langle \psi_0 | H_0 | \psi_0 \rangle + \langle \psi | W | \psi \rangle \leq \langle \psi | H | \psi \rangle \leq \langle \psi_0 | H_0 | \psi_0 \rangle + \langle \psi_0 | W | \psi_0 \rangle. \tag{7.4}$$

This can be rewritten in terms of $g(r)$, the rdf for the total system, and $g_0(r)$ that of the reference system,

$$\frac{E_0}{N} + \frac{\rho}{2} \int g(r) \, w(r) \, d\vec{r} \le \frac{E}{N} \le \frac{E_0}{N} + \frac{\rho}{2} \int g_0(r) \, w(r) \, d\vec{r} \, . \quad (7.5)$$

The r.h.s. of (7.5) is the energy obtained from first order perturbation theory. A complete test of this perturbation theory would require the knowledge of the "exact" solution of the many-body problem both for the reference and the full potential. In view of the success of the Jastrow approximation in the hard-sphere case, we use that approximation consistently in our test of the validity of the first-order perturbation theory.

We have thus performed, in the case of the Lennard-Jones potential at normal density of liquid helium, a series of Monte Carlo computations with a two-body Jastrow factor of the form[7,8]

$$f(r) = e^{-(b/r)^5}$$

We choose for the Lennard-Jones potential the constants[17] $\varepsilon = 10.22°$, $\sigma = 2.556$ Å appropriate to He[4]. The normal density of liquid helium corresponds to $\rho = 0.3648 \, \sigma^{-3}$.

Then the ground state of the total system is obtained
as the minimum of $\langle T + V \rangle$ as a function of b, the ground
state of the reference system as the minimum of $\langle T + V_0 \rangle$.
In this last case the first-order term is also obtained.

We thus obtain

$$E/N = - 5.80 \pm 0.08 \; ^\circ K$$

for

$$b = 1.17(2) \pm 0.01 \; \sigma \; ;$$

and

$$E/N = 17.90 \pm 0.08 \; ^\circ K$$

for

$$b = 1.17(6) \pm 0.01 \; \sigma \; ;$$

and

$$\langle W \rangle /N = - 23.78 \pm 0.05 \; ^\circ K \; .$$

The errors of the Monte Carlo computation remain
large even for the rather precise computation reported here.
Within these errors it is seen that the minimum of $\langle H_0 \rangle$ and
$\langle H \rangle$ are obtained for values of b which are very close as
required for validity of the theory.

Using the data of Table 2 and the set of inequalities (7.5) we can therefore set an upper bound of the order of 0.1°K to the sum of higher order terms in the perturbation theory. We can also state that, due to the closeness of the upper and lower bounds on the energies, $g_0(r)$ and $g(r)$ should be close to each other.

The perturbation theory is therefore seen to work at least as well in the present case as for dense classical liquids. The physical reason for this success is however rather different. In the classical case the good convergence of the perturbation is restricted to the dense states. There, due to the repulsive cores, the particles have little chance to move so that the fluctuations of the perturbing potential remain small. In the quantum fluid, the density is relatively small. The fluctuations are avoided because of the tightness of the wave function: in order to reduce the kinetic energy the particles must keep away from each other as much as possible.

8. Treatment of the Reference System

Our goal is to replace the reference system by a suitably chosen hard sphere system. In the case of classical liquids this replacement is not entirely simple because the particles tend to crowd near their core, so that some account must be taken of the shape of the repulsion.[18] Because in the quantum case the particles must stay away from each other, the rdf will be small wherever the repulsive potential is not zero, so that all shape dependence should be negligible. We thus anticipate that the diameter a will be determined as the scattering length a corresponding to $v_0(r)$ and that the energy of the total system will be given by the first order perturbation formula

$$ E = E_H + \frac{\rho N}{2} \int d\vec{r}\ w(r)\ g_H(r/a)\ , \qquad (8.1) $$

where E_H and g_H are respectively the energy and the rdf of the hard-sphere gas of density ρ and diameter a.

Let us consider again the Lennard-Jones potential with parameters given above. Integration of the Schrodinger equation yields

$$ a = 0.8368\ \sigma\ . $$

The normal density of liquid corresponds to $\rho a^3 = 0.2138$. Using the variational results of section 5 we obtain

$$\frac{E_H}{N} = 17.8 \pm 0.1^\circ \text{ K}$$

$$\frac{<W>}{N} = -23.56 \pm 0.1^\circ \text{ K}$$

We therefore obtain for the total energy $-5.76 \pm 0.15^\circ$ K.
A comparison of these results with the variational results
obtained in the preceding section shows   excellent
agreement.

We shall now proceed to give some theoretical justifica-
tion for the basic expression (8.1).

We shall first introduce an approximation for the rdf.

Let us write in the hard-sphere case

$$g_H(x) = \psi_H^2(x) \ y_H(x) \qquad (8.2)$$

where $\psi_H(x)$ is the solution of the two-body hard sphere
problem at zero energy

$$
\begin{aligned}
\psi_H(r/a) &= \frac{r-a}{r} \ , & r \geq a \\
&= 0 \ , & r < a
\end{aligned}
\qquad (8.3)
$$

$y_H(r/a)$ then is a smooth function of r at the core.
We shall assume that we can write

$$g_0(r) = \psi_0^2(r/a) \ y_H(r/a) \qquad \text{(Assumption A)} \qquad (8.4)$$

where $\psi_0(r/a)$ is a function of r which is equal to
$\psi_H(r/a)$ except near the core. We anticipate that $\psi_0(r/a)$

is the zero-energy solution of the two-body Schrodinger equation with the potential $v_0(r)$.

Assumption A is justified on physical grounds by the idea that only for close two-body encounters is $g_0(r)$ different from the rdf of a hard-sphere gas with a suitably chosen diameter.

Assumption A is not sufficient to determine the kinetic energy. In order to calculate it we must explicitly use the Jastrow approximation. This requires a new assumption. We shall write for the Jastrow factor $f_0(r)$:

$$f_0(r) = \psi_0(r/a) \, S_H(r/a) \quad \text{(Assumption B)} \quad (8.5)$$

where:[4]

$$S_H(x) = f_H(x)/\psi_H(x)$$

$$= \frac{x}{x-1} \tanh \frac{x^m-1}{b_H^m} \quad (8.6)$$

$S_H(x)$ is a smooth function of x at the core.

We shall now see how these two assumptions are connected. It will turn out that the effective expansion parameter of the development of the reference system around hard spheres (in the Jastrow approximation at least) is

$$\rho \, \varepsilon^3 = \rho \, a^3 \int d\vec{x} \, \Delta(x) \quad (8.7)$$

where

$$\Delta(x) = \psi_0^2(x) - \psi_H^2(x) \quad (8.8)$$

is negligibly small except in the region of the core.
For instance at the normal density of helium ($\rho_0 = 0.3648 \ \sigma^3$),
with the above LJ potential it is found that $\rho\varepsilon^3$ is
equal to 0.65×10^{-4}.

The smallness of this parameter explains why we have
replaced in (8.1) the rdf of the reference system,
expected to be given by (8.4) by its hard-sphere
approximation. For the same reason, Assumption B
entails assumption A. Let $g_0(r)$ be the rdf calculated
using assumption B. With the help of the superposition
approximation, we obtain

$$\hat{g}_0(r) = \psi_0^2(\tfrac{r}{a}) \ y_H(\tfrac{r}{a}) \ [1 + \rho a^3 \int d\vec{x}' \ g_H(x') \ \Delta(x')$$

$$\times \ [g_H(x-x')-1] + O(\rho^2\varepsilon^6)] \ . \qquad (8.9)$$

$$r = xa$$

Using the fact that $\Delta(r)$ is concentrated at the core,
we have

$$\delta \ g_0(r) \ = \ \hat{g}_0(r) - g_0(r)$$

$$= \ \rho\varepsilon^3 g_0(r) \ y_H(1) \ \phi(\tfrac{r}{a}) \qquad (8.10)$$

where

$$\phi(x) \ = \ \frac{2\pi}{x} \int\limits_{\sup\{|x-1|,0\}}^{x+1} dx'(g_H(x')-1) \ x' \ . \qquad (8.11)$$

We find that, at the normal density of liquid helium
$|\delta g_0(r)|/ \ g_0(r)$ is smaller than 3×10^{-3}.

Using Assumptions A and B, the energy of the reference system can easily be cast in the form

$$E_0 = \frac{N\rho}{2} \int d\vec{r} \; (\frac{\hbar^2}{4m} \nabla^2 \log f_0(r) + v_0(r)) \; \psi_0^2(\frac{r}{a}) \; y_H(\frac{r}{a})$$

$$= E_H + E_1 + E_2 \; . \tag{8.12}$$

There E_H is the energy of the hard-sphere system with density ρ and diameter a;

$$E_1 = - \frac{N\rho\hbar^2}{4ma^2} \int d\vec{x} \; \nabla x^2 \log S_H(x) \; (\psi_0^2(x) - \psi_H^2(x)) \tag{8.13}$$

is of order $\rho\epsilon^3$ and can be safely neglected.

$$E_2 = \frac{N\rho a^3}{2} \int d\vec{x} \; \phi[\psi_0] \; y_H(r) \tag{8.14}$$

where

$$\phi[\psi_0] = v_0\psi_0^2 - \frac{\hbar^2}{2m} [\psi_H^2 \nabla^2 \log \psi_H - \psi_0^2 \nabla^2 \log \psi_0]. \tag{8.15}$$

$\phi[\psi_0]$ is seen, a posteriori, to be sharply concentrated in the region of the core. We can therefore write

$$E_2 \simeq \frac{\rho a^3}{2} y_H(1) \int d\vec{x} \; \phi[\psi_0] \; . \tag{8.16}$$

If we now minimize the energy with respect to ψ_0, we find that this function obeys the Euler equation:

$$(- \frac{\hbar^2}{m} \nabla^2 + v_0) \psi_0 = 0 \; . \tag{8.17}$$

Furthermore, at the minimum, E_2 as given by (8.16) is seen to vanish. A direct computation shows that, at normal density $E_1 + E_2$ is smaller than .05°K.

We now see that assumption B has been used as an intermediate step in the reasoning. Its explicit use appears only in the evaluation of correction terms which are shown to be negligible. Furthermore it will be shown in the next section that assumption B is very well justified.

9. Remarks on the Variational Problem

Assumption B, if taken literally, has the advantage of providing a Jastrow wave function for the reference system which, given the variational solution of the hard-sphere problem, involves no new parameter. In order to put this remark in practical use, we must give an analytical form for $\psi_0(x)$. Putting

$$u_0(x) = x \, \psi_0(x) \qquad (9.1)$$

we have found the following fit for the solution of the Schrodinger equation (8.17) with the Lennard-Jones constants defined above:

$$u_0 = (c_0 + c_1(x-1)) \exp(-w(\frac{1}{x^5} - 1)) \quad \text{for } x \le 1$$

$$\qquad\qquad\qquad\qquad\qquad\qquad\qquad\qquad\qquad (9.2)$$

$$u_0 = x - 1 + c_0 (1+c_2(x-1)^2) \exp(-k(x-1)) \text{ for } x>1$$

where

$$w = \frac{8\pi}{10\Lambda^* a^5}$$

$$\Lambda^* = \sqrt{\frac{\hbar^2}{m\sigma^2\varepsilon}} = 2.67$$

$$c_0 = 0.04118$$

$$c_1 = 0.0515$$

$$c_2 = -30.18$$

$$k = 11.56 \; .$$

We can use (8.5) with (8.6) and (8.17) to perform a Monte Carlo calculation of the usual type. We have to compute

$$E_0 = <T + V_0> \qquad (9.3)$$

Using the Schrodinger equation it is easily seen that

$$T(r) + v_0(r) = \frac{v_0(r)}{2} + \frac{\hbar^2}{2ma^2} \left[\frac{1}{2} (\frac{u_0'}{u_0})^2 - \frac{u_0'}{u_0} \frac{1}{x} \right] - \frac{\hbar^2}{2ma^2} \nabla_x^2 \log S_H$$

$$(9.4)$$

We find, at normal density

$$\frac{E_0}{N} = 18.03 \pm 0.1 \,^\circ K$$

$$\frac{W}{N} = -23.51 \pm 0.1 \,^\circ K$$

We thus obtain $E = -5.5 \pm 0.2 \,^\circ K$. This should be compared with the value $E = -5.73 \pm 0.1$ obtained variationally, and with the value $E = -5.8 \pm 0.2$ obtained from first order perturbation theory. We see that the agreement is excellent.

In the past, the variational computations of the energy of helium-like systems have all been performed with Jastrow functions of the form $e^{-(b/r)^m}$, [7,8] or functions very nearly of that form.[19,20] All the functions hitherto used have the property of tending rather slowly towards 1 for large values of r. A Jastrow function of the form (8.5) is very different, and we wish to investigate its use in calculating the energy of the quantum Lennard-Jones

fluid. It depends on one variational parameter only which is the equivalent hard-sphere diameter a. For $\psi_0(r/a)$ we shall use the analytical expression provided by eqs. (9.1) and (9.2). With this Jastrow function we have performed Monte Carlo computations for 256 particles for various values of the diameter. The results are summarized in Table 3.

A propos of the energies for the reference system, given in the second column of that table, a remark is in order: In general, for arbitrary values of a, the Jastrow function (9.2) is no longer a solution of the Schrodinger equation. The Laplacian of the Jastrow function must therefore be evaluated directly, instead of using (8.17). Because (9.2) gives an excellent fit, this entails no practical difference.

The variational computation yields for the reference system an energy of 17.8^0 K, which is consistent with and not significantly below the value 17.9^0 K obtained with the function $\exp[-(b/r)^5]$. The energy minimum is obtained for a = 0.82 (5). This is close to (but a little smaller than) the scattering length, especially if one realizes that at the minimum the energy varies but little with a. Assumption B of the preceding section is well verified.

The total energy per particle is equal to -5.82 ± 0.1^0 K. This turns out to be little different from the energy obtained with the Jastrow wave function $\exp[-(b/r)^5]$, i.e. -5.73 ± 0.1^0 K.

Taking into account the usual tendency to underestimate the errors in Monte Carlo computations, we do not find convincing evidence in the literature that a lower value of the energy can be obtained with a Jastrow wave function (at least when long wave length phonons are not included). The form (9.2) for the Jastrow function is sounder than the usual $e^{-(b/r)^m}$ because it exhibits hard sphere features which are the most important characteristics of liquid helium. We compare in Figure 3 the structure factors obtained with these two different Jastrow factors. The overall agreement is good. As expected, with a hard-sphere-like Jastrow factor, one gets a higher main peak in the structure factor than with a smoother trial function.

10. Results of the Perturbation Theory

We shall apply perturbation theory to the case of the Lennard-Jones potential. As in that case complete and reliable results exist only for short range Jastrow functions, we shall as a first step use, in order to be consistent, the corresponding variational hard-sphere results neglecting phonons in both cases. The corrections will be made afterwards.

We use the values of the variational rdf listed in Appendix A in order to calculate, with the help of formula (8.1), the energy of the quantum fluid composed of Lennard-Jones molecules. This is compared in Table 4 with the variational results of ref. 8 for the liquid and with those of Hansen and Pollock[10] for the solid. The statistical errors on the energy and rdf of the hard-sphere gas entails an error on the energy obtained from perturbation theory, which is difficult to estimate because there is clearly a correlation between the errors on the zeroth and first order terms. For $\rho a^3 = 0.2138$ we have made two independent runs, the results of which are compared in Table 4. The final energies differ by 0.1 ° K. The error in the solid region is larger because there we replaced the rdf for distances larger than 2.4 a by 1; the effect of this cut-off is clearly not negligible.

We expect the perturbation theory to break down for low densities where one may get large density fluctuations

without increasing the kinetic energy much and in the high
density solid region where the hard-sphere approximation
must break down. There is, in contrast with the classical
case,[21] a large domain of density where the perturbation
theory with the hard-sphere approximation works well in the
case of the solid. The reason for this success is that
in the quantum case solidification occurs at a quite low
density because the particles must stay away from the core
of their neighbors, and the details of the repulsion are
not seen. As a whole, we do not see in Table 4 any clear
discrepancy between the perturbation results and the results
obtained variationally. There may be an exception to that
statement for the lowest liquid density ($\rho = 0.167$) where
the rather large discrepancy may be due to our neglect of
density fluctuations, and for the highest solid density where
the large discrepancy between the perturbation and variational
results may be significant. As a whole it appears that
the perturbation theory applies in a density domain which
is remarkably large.

Now that the validity of the perturbation theory has
been checked within the framework of the Jastrow approximation,
we shall replace the approximate HS results by "exact" ones.
There are three kinds of corrections which all tend to lower
the energy.

1) The replacement of the variational HS energies by "exact" ones, as computed for 256 particle systems. This appears to be the leading correction.

2) The use of "exact"   instead of variational rdf in the computation of the first-order term. This correction is negligible in the solid region and very small (of the order of 0.05°) in the fluid region.

3) The phonon correction is small but not completely negligible. With the value of the HS diameter which has been chosen, and with the Michels · constants for the LJ potential, we obtain for the velocity of sound in the hard-sphere system the value 295 m/s for the equilibrium density of liquid helium. This is not far from the experimental value (239 m/s). Due to the small size of the phonon correction, it is rather irrelevant which value we use.

The perturbation results thus obtained are shown in Table 5 and compared with the experimental values.[22,23] It is seen that, within the estimated error, which is by no means small, there is no clear discrepancy except at the highest solid density where the Lennard-Jones potential clearly gives energies which are too low as already known from the work of Hansen and Pollock.[10] We can obtain a confirmation of these results in the following way: as we have seen, the correction to be applied to the variational results is essentially that in the kinetic energy. We can

therefore estimate the exact energy by adding to the variational LJ energies a term

δE = exact energy of the equivalent HS system minus variational energy of the HS system.

In this process, we use smoother data than in the straight perturbation theory. The LJ variational data are quite precise and smooth, and δE can also be smoothed. The values of δE which are used are given in Table 6 and the energies thus obtained are given in column 5 of Table 5. They are entirely compatible with the perturbation energies and with experiment (except at very high density).

We did not try to determine from the above data the transition and equilibrium densities. They are obviously compatible with the experimental data, within a large uncertainty which may amount to 10%.

11.   The Hard Sphere Model

In the preceding sections, the close relationship between the reference system and the hard-sphere fluid has been exhibited. It has moreover been shown that the attractive forces change the structure only a little. In particular, it has been demonstrated in section 9, on the basis of variational computations, that a hard-sphere-like Jastrow function is perfectly acceptable for the description of the full LJ fluid. Still within the variational framework, we can obtain a further test of the validity of this hard sphere representation by comparing the off-diagonal long-range order parameter obtained[7,8] for the LJ fluid at normal density (with the $e^{-(b/r)^5}$ Jastrow factor), i.e. $n_0 = 0.105 \pm 0.005$, with the HS variational value at $\rho a^3 = 0.2138$ where we find $n_0 = 0.093 \pm 0.033$.   These values are clearly compatible. Last, we may try the solidification criterion used in the classical case:[24] the real system solidifies when the equivalent HS system does. The solidification density of the HS system in the variational approximation is obtained for $\rho a^3 = 0.23 \pm 0.01$. This gives for the LJ system $\rho \sigma^3 = 0.39 \pm 0.2$, which should be compared with the value $\rho \sigma^3 = 0.38$ obtained through the variational computation made   directly in the LJ system.[11]

Let us now go beyond the Jastrow approximation. In Figure 4 we show the "exact" $S(k)$ appropriate to the normal density of liquid helium. We take for the full LJ system the same equivalent hard-sphere density $\rho a^3 = 0.2138$ corresponding to a diameter $a = 0.8368 \, \sigma$ as in the case of the reference system. This choice is motivated as follows: we know from the computations of section 9 that the attractive forces have the tendency to reduce the equivalent diameter to a value around $a = 0.81 \, \sigma$. On the other hand, we know that in order to describe real helium more realistic potentials than the usual LJ potential used in this study should be used such as the potential due to Beck[25] or the modified Lennard-Jones potential (LJ2) considered by Hansen and Pollock.[10] These potentials have a wider core than the LJ potential with Michels constants. They both yield the value $a = 0.86\sigma$ as the equivalent hard-sphere diameter for the reference fluid. We thus see that keeping the value $a = 0.8368\sigma$ realized a compromise between the above two effects.

The determination of the "exact" $S(k)$ involves some manipulations which should be indicated. For $\rho a^3 = 0.2$, we can compute precisely the difference between the exact and variational rdf. This difference is scaled and added to the variational rdf at $\rho a^3 = 0.2138$. In order to get the Fourier transform of the rdf, we have obtained its value beyond $r = 2.4a$ by using the Ornstein-Zernike relation

and the assumption that, for large r, the direct correlation function is negligible.[8] The phonon contribution is then calculated as indicated in section 6, using for the sound velocity the experimental value and for the cut-off wave vector the value $k_c = 0.3 \, a^{-1}$ that leads to the energy minimum.

The structure factor thus determined is compared in Figure 4 to experimental results obtained by X-ray scattering. Hallock's data[26] have been used for $k < 1.1 \, \overset{\circ}{A}^{-1}$ (ka < 2.3). Achter and Meyer's results[27] are shown for higher values of k. It is seen that, at low k our results agree well with those of Hallock although they show the shoulder predicted by Miller, Pines and Nozieres[28] a little more. We may note that this shoulder was not observed by Achter and Meyer whose results may differ from Hallock's by as much as 10%. In the k region corresponding to the rise of the first peak, the experimental and theoretical results agree quite well. The position of the first peak and the zeros in S(k)-1 differ markedly. We note however that this disagreement is no longer present when one considers the results obtained from neutron scattering by Henshaw.[29] There however the first peak rises to a much higher value than in Figure 4.

In order to get more insight into the origin of the discrepancy at large k, we reexamine the experimental data used in Figure 4. The rdf obtained from these results by

Fourier transform is not strictly zero inside the core. If we correct this rdf by imposing simply that it vanish for $r \lesssim a$, the structure factor that we obtain by Fourier transform is no longer identical with the experimental one. We can impose a compatibility with experiment in the low k region (including the first peak and a strict vanishing of the rdf inside the core if we iterate the procedure described above, based on a succession of Fourier transforms. In this way, a self-consistent structure factor is reconstructed, with admittedly some measure of arbitrariness. The results are shown in Figure 4. It is seen that the agreement with the hard sphere structure factor is somewhat improved. We believe the remaining discrepancy to be due more to the errors in the hard-sphere rdf and the experimental structure factor than to a defect in the model.

The "exact" ODLRO parameter is estimated as $n_0 = 0.095 \pm .001$ at $\rho a^3 = 0.2$. It is very different from the recent estimate[30] of $n_0 = 0.0241 \pm .01$ which is obtained indirectly from experiment at 1.2 ° K.

Last, we examine the solidification criterion. The freezing density for hard spheres $\rho a^3 = 0.25 \pm 0.01$ yields the value $\rho \sigma^3 = 0.427$. At the solidification density, the main peak of the hard sphere structure factor reaches the value 1.40 which should be compared to the value 2.85 in the classical case.[24] A value of the order of 1.40 should therefore be the maximum value reached by the structure factor of liquid helium at very low temperature in the whole fluid range.

We tabulate the radial distribution function for the hard sphere Bose fluid as computed by the Monte Carlo integration of the Schrodinger equation and by the variational method with the Jastrow factor[4]

$$f(r) = \tanh \ [(r^m - 1)/b^m] \ .$$

Results are given at $\rho a^3 = 0.2$, 0.244, and 0.27. The numbers tabulated as g are in fact average values over the interval ending in the r. That is

$$g(r_n) = \int_{r_{n-1}}^{r_n} r^2 g(r) \ dr \ / \int_{r_{n-1}}^{r_n} r^2 \ dr \ .$$

We estimate the statistical error of the values as less than 2% except for the first few entries which have errors of 5-10%. A systematic error of a few percent at the peak of $g(r)$ is possible owing to incomplete convergence of the iteration process used in the calculation.

The problem of solid He^3 is treated exactly as above. As long as we neglect the (small) exchange effects, the only difference with He^4 lies in the lighter mass of He^3. Schiff[12] has calculated the effective diameter of the reference part of the LJ potential in the He^3 case and found the value 0.823 σ. He has shown that, in the variational framework, the perturbation theory works as well as in the solid He^4 case. Here we use the results of Schiff, but with "exact" results for the HS boson solid instead of variational results. As above, we give both the results obtained by a straight application of perturbation theory and the estimate obtained from correcting the variational results for the difference between "exact" and variational HS results. Both methods lead to energies which agree, within the rather large errors, with experiment, as in the He^4 case.

For the liquid state, the antisymmetry of the wave function must be taken into account. In the absence of "exact" hard sphere results in the fermion case, one is led to rely on the Wu-Feenberg approximation:

$$\psi_{He^3}(\vec{r}_1 \ \cdots \ \vec{r}_N) \ = \ \psi_B(\vec{r}_1 \ \cdots \ \vec{r}_N) \ \psi_F(\vec{r}_1 \ \cdots \ \vec{r}_N) \ ,$$

where ψ_B is the solution of the mass 3 boson problem and ψ_F is the appropriate Slater determinant of plane waves. As Wu and Feenberg have shown, if the ground state

properties of the boson system are known, the energy of the He^3 fluid can be calculated by making a cluster expansion of the determinant. This expansion seems to converge quite well. For the Lennard-Jones potential variational results are available.[9] In that case, Schiff has shown that the perturbation methods also work quite well. Schiff's results rely on three assumptions: (1) variational results are used for the hard-sphere boson fluid.

(2) The Lennard-Jones potential is a good approximation for the He - He interaction.

(3) The Wu-Feenberg ansatz is a good approximation.

Here (Table 8) we correct for (1) by using "exact" hard sphere results. We know from the He^4 study that the error entailed by the use of the LJ potential is small (less than 0.5°). The very clear discrepancy revealed in Table 8 in the He^3 is then largely due to the use of the Wu-Feenberg ansatz, whose effect amounts to an overestimation of the energy by at least 1 °.

References

1. N. N. Boglioubov, J. Phys. USSR $\underline{11}$, 23 (1947).

2. T. D. Lee and C. N. Yang, Phys. Rev. $\underline{105}$, 1119 (1957).

3. T. T. Wu, Phys. Rev. $\underline{115}$, 1390 (1959)

    J. B. Aviles, Ann. Phys. (N.Y.) $\underline{5}$, 251 (1958)

    R. Drachman, Phys. Rev. $\underline{131}$, 1881 (1963).

4. J. P. Hansen, D. Levesque and D. Schiff, Phys. Rev. $\underline{A3}$, 776 (1971).

5. M.H. Kalos, Phys. Rev. $\underline{A2}$, 250 (1970).

6. J. D. Weeks, D. Chandler and H. C. Andersen, J. Chem. Phys. $\underline{54}$, 5237 (1971).

7. W. L. McMillan, Phys. Rev. $\underline{138}$ A 442 (1965).

8. D. Schiff and L. Verlet, Phys. Rev. $\underline{160}$, 208 (1967).

9. J. P. Hansen and D. Levesque, Phys. Rev. $\underline{165}$, 293 (1968).

10. J. P. Hansen and E. L. Pollock, Phys. Rev. $\underline{A5}$, 2651 (1972).

11. The ratio of the multivariate anisotropic distribution to a distribution isotropic for each sphere may be regarded as a weight factor. This factor times the ratio $\psi_J(R)/\psi_J(R')$ is the branching ratio used in a move from point R' to point R. Clearly it is possible to make this branching factor arbitrarily close to one, reducing its contribution to the overall variance to zero.

12. D. Schiff, to be published.

13. L. Reatto and G.V. Chester, Phys. Letters $\underline{22}$, 276 (1966).

14. J. Zwanziger, Thesis, Cornell (1972).

15. J. L. Lebowitz, G. Stell and S. Baer, J. Math. Phys. $\underline{6}$, 1282 (1965).

16. H. C. Andersen and D. Chandler, J. Chem. Phys. $\underline{55}$, 1497 (1971).

17. J. de Boer and A. Michels, Physica $\underline{5}$, 945 (1938).

18. L. Verlet and J. J. Weis, Phys. Rev. $\underline{A5}$, 939 (1972).

19. D. Levesque, Tu Khiət, D. Schiff and L. Verlet, Orsay Report 1965 (unpublished).

20. R. D. Murphy, Phys. Rev. $\underline{A5}$, 331 (1972).

21. J. J. Weis, Thesis, Orsay (1973).

22. P. R. Roach, J. B. Ketterson and C. W. Woo, Phys. Rev. $\underline{A2}$, 543 (1970).

23. G.C. Straty and E.D. Adams, Phys. Rev. $\underline{169}$, 232 (1968).

24. J.P. Hansen and L. Verlet, Phys. Rev. $\underline{184}$, 151 (1969).

25. D. E. Beck, Mol. Phys. $\underline{14}$, 311 (1968).

26. R.B. Hallock, Phys. Rev. $\underline{A5}$, 320 (1972).

27. E.K. Achter and L. Meyer, Phys. Rev. $\underline{188}$, 291 (1969).

28. A. Miller, D. Pines and P. Nozieres, Phys. Rev. $\underline{127}$, 1452 (1962).

29. D.G. Henshaw, Phys. Rev. $\underline{119}$, 9 (1960).

30. H. A. Mook, R. Scherm, and M. K. Wilkinson, Phys. Rev. $\underline{A6}$, 2268 (1972).

31. F. Y. Wu and E. Feenberg, Phys. Rev. $\underline{122}$, 739 (1961).

Table 1

State	ρa^3	E_1	phonon correction	E_0
fluid	0.166	4.24 $\pm$ .05	– 0.09	4.15 $\pm$ .05
	0.200	5.80 $\pm$ .05	– 0.11	5.69 $\pm$ .05
	0.244	8.28 $\pm$ .09	– 0.14	8.14 $\pm$ .09
	0.270	10.65 $\pm$ .07	– 0.15	10.50 $\pm$ .07
F.C.C. crystal	0.244			8.50 $\pm$ .05
	0.270			10.12 $\pm$ .04
	0.300			12.27 $\pm$ .07
	0.400			21.26 $\pm$ .07
	0.500			34.45 $\pm$ .25

Energies in units of $\hbar^2/ma^2$ for the ground state
of the quantum hand sphere fluid and F.C.C. solid.
For the fluid, E_1 is the result of the Monte Carlo
integration of the Schrodinger equation for a system
of 256 particles. The phonon correction to an infinite
system is obtained by the method of section 6.
For the crystal the results for 256 particles are given
with no corrections. Errors are estimates of the
standard deviation.

Table 2

b	$(\langle T\rangle/N)^\circ$	$(\langle V_0\rangle/N)^\circ$	$(E_0/N)^\circ$	$(\langle W\rangle/N)^\circ$	$(E/N)^\circ$	n
1.16	13.59	4.45	18.04	-23.83	- 5.79	650000
1.17	13.95	4.09	18.04	-23.80	- 5.76	650000
1.18	14.30	3.60	17.90	-23.76	- 5.86	400000
1.20	15.07	3.06	18.15	-23.68	- 5.53	650000

Energies obtained variationally for the
reference system (column 4) and for the system
with the full LJ potential (column 6).
n is the total number of configurations.
The statistical error on the kinetic and
potential energies is of the order of 0.05 °.
The error on the total energies is   about 0.08°.

Table 3

a	$(E_0/N)°$	$(E/N)°$	n
0.75	20.64 ± 0.08	− 3.64 ± 0.12	600 000
0.80	18.04 ± 0.04	− 5.78 ± 0.06	2 500 000
0.82	17.84 ± 0.04	− 5.81 ± 0.06	2 300 000
0.8368	18.04 ± 0.04	− 5.48 ± 0.06	2 000 000
0.86	18.40 ± 0.04	− 4.93 ± 0.06	2 300 000

Variational energies for the LJ system
using the Jastrow factor defined by (9.1) and (9.2).
Column 1: equivalent hard sphere diameter.
Column 2 and 3: energy of the reference system
and of the complete system respectively.
Column 4: total number of configurations in the
Monte Carlo computation.

Table 4

ρa^3	$\rho \sigma^3$	$E_H(\frac{ma^2}{N\hbar^2})°$	$(E_H/N)°$	$(\langle W\rangle/N)°$	$(E/N)°$	$(E_{var}/N)°$
0.167	0.283	4.32±0.1	11.38	-16.64	- 5.26±0.2	-5.67±0.1
0.2	0.341	6.01±0.1	15.83	-22.09	- 6.16±0.2	-5.91±0.1
0.2138	0.364	6.85±0.1	18.05	-23.89	- 5.84±0.2	-5.73±0.1
0.2138	0.364	6.75±0.1	17.80	-23.56	- 5.76±0.2	-5.73±0.1
0.234	0.4	7.92±0.1	20.87	-26.27	- 5.40±0.2	-5.25±0.1
0.244	0.416	8.86±0.1	23.33	-28.44	- 5.11±0.4	-4.97±0.2
0.27	0.461	10.6 ±0.1	27.92	-32.73	- 4.79±0.5	-4.75±0.2
0.3	0.512	12.69±0.1	33.40	-36.50	- 3.10±0.6	-3.87±0.3
0.35	0.597	16.8 ±0.2	44.20	-44.56	- 0.36±0.8	-1.4 ±0.4
0.4	0.683	21.9 ±0.2	57.70	-54.85	2.87±1	3.2 ±0.5
0.5	0.853	35.5 ±0.3	93.5	-66.02	27.5 ±2	22.8 ± 1

Energies of the LJ system computed within
the Jastrow approximation. Column 6 gives
the result of the perturbation theory.
Column 7 gives the variational results.
The upper half of the table refers to fluid
states, the lower half to solid states.
For the density $\rho a^3 = 0.2138$, the results
of two independent Monte Carlo runs have been
given for comparison.

Table 5

ρa^3	$\rho\sigma^3$	$(E_{var}/N)°$	$(E_{pert}/N)°$	$(E_{est}/N)°$	E_{exp}/N
0.167	0.283	-5.67 ± 0.1	-5.72 ± 0.2	-6.13 ± 0.2	
0.2	0.341	-5.91 ± 0.1	-7.14 ± 0.2	-6.77 ± 0.2	(-7.09)
0.244	0.416	-5.02 ± 0.1	-6.50 ± 0.2	-6.67 ± 0.2	-6.84
0.244	0.416	-4.97 ± 0.2	-6.11 ± 0.4	-5.97 ± 0.4	(-5.5)
0.27	0.461	-4.75 ± 0.2	-5.79 ± 0.5	-5.75 ± 0.5	-6.08
0.3	0.512	-3.87 ± 0.3	-4.10 ± 0.6	-5.00 ± 0.6	-5.3
0.4	0.683	3.2 ± 0.5	1.2 ± 1	1.5 ± 1	2.1
0.5	0.853	22.8 ± 1	24.8 ± 2	20.1 ± 2	26

Results of perturbation theory. Column 4:
perturbation energies using hard sphere results
Column 5: Estimated energies obtained by adding
to the variational LJ results of column 3 the
hard sphere correction δE given in Table 6.
The upper half of the table refers to fluid states,
the lower half to solid states.

Table 6

ρa^3	E_{exact}/N	E_{var}/N	$\delta E/N$
0.166	4.15	4.32	0.17
0.2	5.69	6.01	0.32
0.244	8.14	8.80	0.66
0.244	8.50	8.86	0.38
0.27	10.12	10.50	0.38
0.3	12.27	12.65	0.43
0.4	21.26	21.9	0.64
0.5	34.45	35.5	1.05

Smoothed difference $\delta E/N$ between the "exact" energy per particle of the hard sphere system and its variational estimate. Energies in units of $\hbar^2/ma^2$.

Table 7

$$\rho a^3 = 0.2$$

r	g_s	g_v	r	g_s	g_v	r	g_s	g_v	r	g_s	g_v
1.10	0.049	0.044	2.20	1.025	1.012	3.30	1.045	1.021	4.40	1.016	0.995
1.20	0.239	0.259	2.30	0.949	0.969	3.40	1.037	1.018	4.50	0.993	0.997
1.30	0.542	0.567	2.40	0.912	0.941	3.50	1.009	1.017	4.60	1.000	1.002
1.40	0.870	0.876	2.50	0.880	0.933	3.60	0.990	1.015	4.70	0.990	0.998
1.50	1.113	1.121	2.60	0.890	0.947	3.70	0.990	1.005	4.80	0.999	1.004
1.60	1.280	1.253	2.70	0.907	0.943	3.80	1.005	0.998	4.90	0.999	1.001
1.70	1.394	1.299	2.80	0.958	0.964	3.90	0.992	0.997	5.00	1.007	1.001
1.80	1.322	1.274	2.90	0.990	0.981	4.00	0.993	0.999	5.10	0.987	1.000
1.90	1.236	1.198	3.00	1.025	0.992	4.10	0.995	0.993	5.20	1.003	1.002
2.00	1.198	1.142	3.10	1.045	1.005	4.20	0.990	0.989	5.30	1.005	1.002
2.10	1.065	1.069	3.20	1.048	1.011	4.30	0.998	0.996	5.40	1.003	1.000

$$\rho a^3 = 0.244$$

r	g_s	g_v	r	g_s	g_v	r	g_s	g_v	r	g_s	g_v
1.10	0.044	0.031	2.20	0.912	0.923	3.30	1.119	1.103	4.40	0.990	0.988
1.20	0.252	0.245	2.30	0.820	0.847	3.40	1.077	1.073	4.50	1.014	1.012
1.30	0.587	0.636	2.40	0.786	0.801	3.50	1.044	1.042	4.60	1.048	1.040
1.40	0.955	1.035	2.50	0.787	0.790	3.60	0.998	1.004	4.70	1.057	1.059
1.50	1.271	1.285	2.60	0.812	0.820	3.70	0.963	0.976	4.80	1.066	1.060
1.60	1.457	1.414	2.70	0.880	0.881	3.80	0.936	0.952	4.90	1.056	1.057
1.70	1.504	1.428	2.80	0.952	0.953	3.90	0.931	0.940	5.00	1.036	1.035
1.80	1.409	1.365	2.90	1.021	1.018	4.00	0.933	0.935	5.08	1.021	1.023
1.90	1.283	1.291	3.00	1.085	1.077	4.10	0.943	0.937			
2.00	1.169	1.162	3.10	1.129	1.110	4.20	0.949	0.952			
2.10	1.029	1.037	3.20	1.131	1.125	4.30	0.969	0.966			

$$\rho a^3 = 0.27$$

r	g_s	g_v	r	g_s	g_v	r	g_s	g_v	r	g_s	g_v
1.05	0.017	0.021	2.05	0.919	0.938	3.05	1.054	1.035	4.05	1.005	1.003
1.10	0.100	0.109	2.10	0.886	0.909	3.10	1.055	1.026	4.10	1.008	1.000
1.15	0.256	0.280	2.15	0.877	0.889	3.15	1.036	1.024	4.15	1.024	1.008
1.20	0.450	0.507	2.20	0.874	0.877	3.20	1.004	1.014	4.20	1.006	1.004
1.25	0.686	0.739	2.25	0.843	0.877	3.25	1.024	1.004	4.25	1.014	0.998
1.30	0.931	0.990	2.30	0.863	0.887	3.30	0.994	1.001	4.30	1.017	1.005
1.35	1.154	1.184	2.35	0.877	0.894	3.35	0.994	1.011	4.35	1.003	1.005
1.40	1.320	1.330	2.40	0.887	0.910	3.40	0.999	0.997	4.40	0.996	1.002
1.45	1.415	1.425	2.45	0.924	0.928	3.45	1.017	0.981	4.45	0.993	1.009
1.50	1.489	1.469	2.50	0.922	0.941	3.50	0.997	0.983	4.50	1.008	1.003
1.55	1.527	1.492	2.55	0.942	0.968	3.55	0.986	0.985	4.55	0.996	1.003
1.60	1.478	1.441	2.60	0.961	0.972	3.60	0.972	0.936	4.60	1.000	0.999
1.65	1.431	1.387	2.65	0.987	1.000	3.65	0.963	0.984	4.65	0.999	0.994
1.70	1.364	1.313	2.70	1.022	1.005	3.70	0.975	0.990	4.70	1.010	1.002
1.75	1.273	1.243	2.75	1.034	1.022	3.75	0.970	0.985	4.75	0.995	0.998
1.80	1.217	1.162	2.80	1.060	1.022	3.80	0.976	0.989	4.80	1.006	0.999
1.85	1.108	1.094	2.85	1.034	1.044	3.85	0.988	1.001	4.85	1.002	0.999
1.90	1.049	1.025	2.90	1.062	1.050	3.90	0.984	0.993	4.90	0.997	0.996
1.95	0.986	1.004	2.95	1.033	1.053	3.95	0.992	0.997	4.91	1.008	0.995
2.00	0.957	0.965	3.00	1.033	1.035	4.00	1.001	0.994			

Radial distribution function for fluid states of the hard sphere boson system calculated by variational method (g_v) and Schrodinger integration (g_s).

Table 8

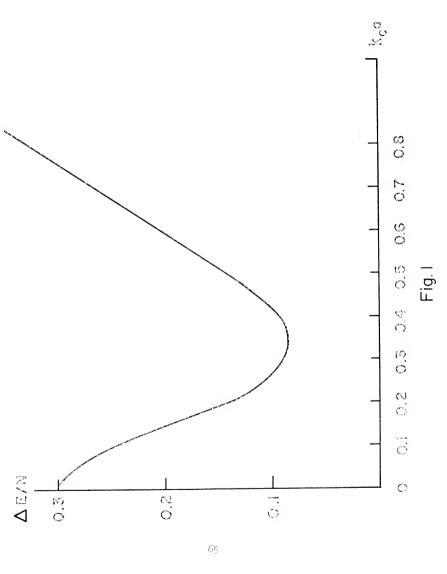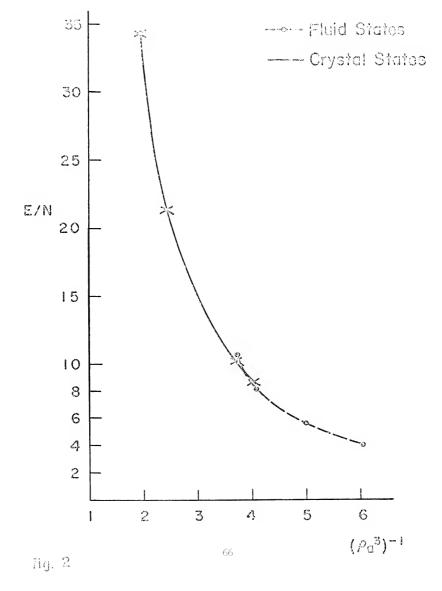| ρa^3	$\rho\sigma^3$	$(E_{var}/N)°$	$(E_{pert}/N)°$	$(E_{est}/N)°$	$(E_{exp}/N)°$
0.167	0.283	-1	-1.2	-1.3	- 2.4
0.2	0.341	0	-0.35	-0.75	- 2.2
0.2138	0.364	0.6		-0.4	- 1.8
0.234	0.4	2.2		0.75	
0.244	0.416	3.2	0.55	1.65	
0.244	0.416	1.5	0.2 ±0.6	0.1 ±0.6	- 0.4
0.27	0.461	3.2	1.8 ±0.8	1.8 ±0.8	1.1
0.3	0.512	5.8	4.2 ±1.0	4.3 ±1.0	4.6
0.35	0.597	11.7		9.8 ±1.2	11.5

Results of the perturbation theory applied to He^3.
Same as in Table 5. The results for the liquid state
have been obtained using the Wu-Feenberg ansatz.

Figure Captions

Fig. 1   Energy shift due to long wavelength phonons in units $\hbar^2/ma^2$, as a function of the cut-off wave vector k_c for the density $\rho a^3 = 0.234$.

Fig. 2   "Exact" energy per particle as a function of $1/\rho a^3$.

Fig. 3   Structure factor for the Lennard-Jones system as given by variational computations at the normal density of liquid helium. Solid curve: Jastrov factor $e^{-(b/r)^5}$ with b = 1.18. Dotted line: hard-sphere-like Jastrow factor as given by (9.1) and (9.2) with a = 0.83.

Fig. 4   Structure factor at the normal density of liquid helium. Solid line: experiment.[27,28] ⊙ ⊙ ⊙ : "reconstructed" experiment as explained in the text. · · · : "exact" hard sphere structure factor.

Fig. I

65

Fig. 2

NOV 16 1973

DATE DUE

COO-3077-35   c.2

Kalos

Helium at zero-temperature
with hard-sphere...

N.Y.U. Courant Institute of
Mathematical Sciences
251 Mercer St.
New York, N. Y. 10012